



Comparison of Energy Consumption of Different Electric Vehicle Power Systems Using Fuzzy Logic-Based Regenerative Braking

Enes Yurdaer¹, Tolga Kocakulak^{2*}

¹Automotive Engineering Department, Faculty of Technology, Gazi University, Ankara, 06500, Turkey

²Vocational School of Technical Sciences, Burdur Mehmet Akif Ersoy University, Burdur, 15100, Turkey

Abstract

One of the disadvantages of electric vehicles that has not yet been overcome is the long battery refueling time. Besides studies to shorten the battery refueling time, increasing the driving range is also a solution to this problem. Different energy saving methods have been tried to increase the driving range. Regenerative braking is one of the best energy-saving methods in electric vehicles. Among several different strategies for regenerative braking, in this study, a fuzzy logic-based regenerative braking strategy is applied to ensure the best regenerative ratio for electric vehicles in any braking case. Moreover, three electric vehicles with different powertrains are modeled in MATLAB/Simulink, and their regenerative braking effectiveness is compared. Inputs of this fuzzy logic controller were determined as the vehicle speed, brake pedal position, and state of charge data; also, three different driving cycles are utilized for simulation. These models are equipped with REMY HVH250-115 electric motor and a battery with a capacity of 80 kWh. As a result, the energy-saving amounts are ordered from the best to the worst as all-wheel drive, front-wheel drive, and rear-wheel drive configurations. Furthermore, the average energy-saving in the all-wheel drive configuration is calculated as 19.11%, in the front-wheel drive configuration is calculated as 9.38%, and in the rear-wheel drive configuration is calculated as 7.93%.

Keywords: Electric Vehicles, Fuzzy Logic, Regenerative Braking, Vehicle Modeling, Powertrain

History

Received: 14.11.2020

Accepted: 23.03.2021

Author Contacts

*Corresponding Author

enesyurdaer@gmail.com, tkocakulak@mehmetakif.edu.tr

Orcid: 0000-0001-8437-9457, 0000-0002-1269-6370

<http://dx.doi.org/10.29228/sciperspective.47590>

1. Introduction

Especially in the last half-century, electric vehicles (EVs) have been brought to the agenda again due to the shortage of fossil fuels and environmentalist attitudes, and studies are being conducted on EVs. Thus, in the near history, EVs became a real rival to conventional vehicles for the first time [1,2].

Up to the present, the most significant disadvantages of EVs compared to the conventional vehicles were limited range and long refueling time [3,4]. However, these studies also led to the development of battery technology and enabled more extended range and relatively shorter refueling time. Therefore, it is considered that usage of conventional vehicles with internal combustion engines will be discontinued in the near future.

Some of the advantages of EVs and their electric motors (EMs) are listed as follows [5-8].

- EMs have high efficiencies and torque value.
- BEVs do not require complex drivetrain design.

- EMs are almost maintenance-free.

- EVs run quite silently, are environmentally friendly and easy to operate.

In addition to these advantages, EVs make regenerative braking possible thanks to their EMs.

In conventional vehicles, braking can be operated only by a mechanical braking system. However, one of the best advantage of EMs is that they can also run as a generator, which enabled the regenerative braking operation.

Regenerative braking is a braking method that uses EM to slow down the vehicle in case of braking. While regenerative braking, EM works in the reverse direction, so that acts as a generator and recharge the battery [9]. Regenerative braking provides [10-13], much better control of braking, effectiveness in stop-and-go driving conditions, less frequently maintenance of mechanical braking system and better energy consumption compared to conventional braking.

Under proper circumstances, 8-25% of energy saving can be produced by regenerative braking. Moreover, regenerative braking is considered as the most attractive strategy for energy saving in EVs because it does not require any sizeable extra equipment [14].

Theoretically, a significant proportion of braking operation can be supplied by regenerative braking. However, a suitable proportion of regenerative braking must be supplied in reality due to driving safety aspects. For this reason, different regenerative braking strategies were created [15,16]. There are two common regenerative braking strategies as serial and parallel strategies [17]. In the parallel strategy, regenerative braking and mechanical braking start simultaneously, and regenerative brake operates until peaks. In the serial strategy, regenerative braking starts before mechanical braking, and the mechanical braking starts only when the regenerative brake peaks [18].

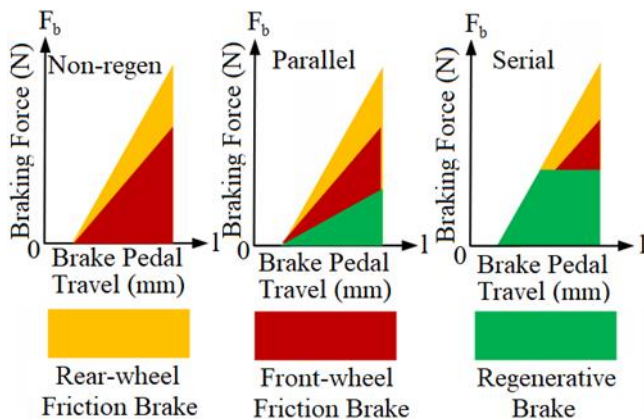


Figure 1. Serial, parallel and non-regen strategies [19]

In the serial strategy, the regenerative braking ratio can be increased compared to the parallel regenerative braking strategy. However, it has a limited part of the total braking in order to avoid problems that might occur in active driving safety systems [20]. This ratio can also be determined by a fuzzy logic controller, which depends on different essential factors such as state of charge (SOC), brake pedal position (BPP), braking force, speed of the vehicle, and temperature of the battery [21,22].

Uses of simple rules and conventional binary logic are insufficient to provide a proper regenerative braking ratio continuously. In contrast, this problem can be overcome by a fuzzy logic controller algorithm because different braking situations can be defined by fuzzy sets and rules [14].

In the regenerative braking strategies, different motor layouts have a considerable effect on energy saving. All-wheel drive (AWD) configurations are quite better than front-wheel drive (FWD) and rear-wheel drive (RWD) configurations in energy-saving comparison because in AWD configurations braking force on both front, and rear axles can be recovered by regenerative braking. Furthermore, FWD configurations are relatively more effective in regenerative braking than RWD configurations because of the location of the vehicle's center of gravity, which is generally close to the front side, and the impact of the inertial force while braking [23,24,25].

Zhang et al. applied a fuzzy logic control to the braking system of a hybrid electric vehicle in order to increase energy saving and regenerative braking efficiency. The energy recovered by regenerative braking was improved by 20% with this fuzzy logic control strategy

[26]. Xu et al. created a fuzzy logic-based regenerative braking strategy for EVs to extend their driving range. Braking force, vehicle speed, SOC, and battery temperature data were determined as the inputs of the fuzzy logic controller. According to experiment results, the maximum driving range was improved by 25.7% compared with non-regenerative braking system [27]. Maia et al. presented a fuzzy logic model of regenerative braking in order to avoid the use of EV on-board sensors. As the average of two different test results, 4.04 kWh energy in reality, and 4.83 kWh energy in the simulation were recovered by regenerative braking [28]. Tao et al. proposed a regenerative braking control strategy based on fuzzy logic for an EV with four in-wheel motors. In order to increase energy-saving efficiency and protect the battery, the SOC variable has been taken into account. Under NEDC, energy recovery efficiency was observed as %17.6 [29]. Xiao et al. proposed a new regenerative braking strategy based on a fuzzy logic controller with SOC, motor speed, and brake strength inputs. This strategy was simulated under different driving cycles and a braking scenario, compared to two different braking strategies. According to the results, the braking performance of the model, which has a fuzzy logic-based regenerative braking strategy, was improved by 21.1% for NEDC [30]. Xin et al. created two different composite brake control strategies based on a fuzzy logic controller for load-isolated electric buses and determined SOC and the braking intensity data as the inputs of this fuzzy logic controller. According to simulation results, the driving range of the vehicle was improved by 7.74%, and the energy-saving rate was improved by 11.05% [31].

In the previous study, which is proposed by Kocakulak and Solmaz, three different hybrid vehicle configurations, pre-transmission parallel hybrid, post-transmission parallel hybrid, and serial hybrid, were modeled. Moreover, their average fuel consumption was calculated and compared for different driving cycles. Also, a fuzzy logic-based regenerative braking strategy was created for these models where the inputs of this fuzzy logic controller are SOC, vehicle speed, battery current and pedal position. Under the ECE 15 driving cycle, the energy-saving amounts were ordered from the best to the worst as series (%14.22), pre-transmission parallel (%11.5), and post-transmission parallel hybrid (%9.95) models [22].

In this study, a fuzzy logic-based regenerative braking strategy is created to ensure the ideal regenerative braking ratio in any braking case for three BEVs with different powertrains (FWD, RWD, and AWD). These three BEV configurations are modeled in MATLAB/Simulink.

Specifications of an average four-door sedan are used as simulation parameters. Also, three different driving cycles (NEDC, WLTP Class 3, and FTP-75) are used as reference speed graphs, and the models are controlled by a PID controller. REMY HVH250-115 electric motor is utilized as the EM, and these models are equipped with a battery with a capacity of 80 kWh.

Thus, some values such as driving range, SOC, average energy consumption (AEC), EM torque, EM power, acceleration, speed, and total distance are calculated and commented. In addition to these data, especially regenerative braking efficiencies of these three configurations are determined and comparatively examined.

2. Material and Method

The BEV models consist of 6 subsystems: driver, EM, driveline, longitudinal resistance forces, battery, and brake.

2.1 Driver Subsystem

Three different drive cycle sources (NEDC, WLTP Class 3, and FTP-75) are utilized as time-dependent reference speed for simulation. The system is controlled by a PID controller, and the vehicle speed is used as feedback data. The output of the PID controller is limited/saturated between -1 and 1. From -1 to 0 is assigned as the BPP, and from 0 to 1 is assigned as the accelerator pedal position (APP). Furthermore, the actual EM torque is obtained by multiplying the APP by the maximum EM torque.

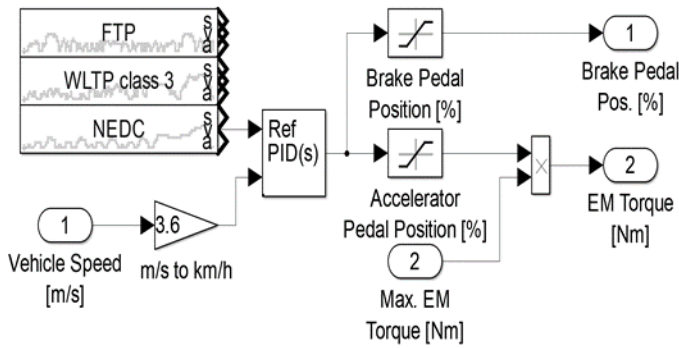


Figure 2. Driver subsystem

2.2 EM Subsystem

It is essential to choose an EM with the proper torque and high-efficiency values for EVs.

In this study, specifications of REMY HVH250-115 Electric Motor are utilized as EM data of the models. The mass of the EM is 57.2 kg, the peak torque is 420 Nm, and the peak efficiency is greater than %95.

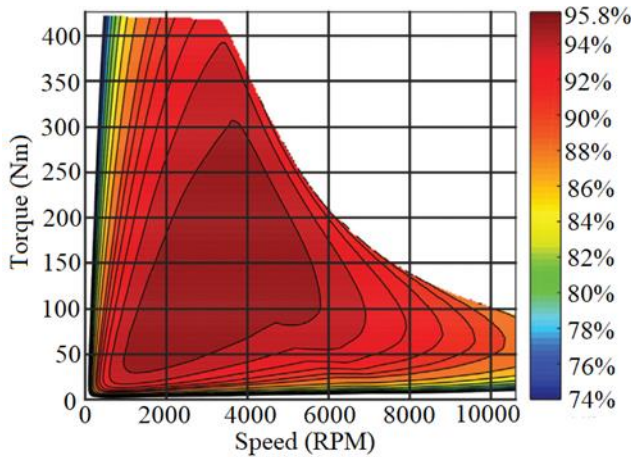


Figure 3. EM Torque Graph [33]

2.3 Driveline Subsystem

Two different equations, to calculate the angular speed of the EM, are obtained for AWD and F/RWD configurations. For F/RWD configurations, the driving force is only transmitted through the

front/rear axle.

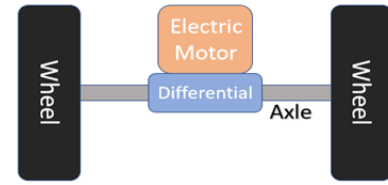


Figure 4. EM layout of F/RWD configurations

For AWD configurations, the driving force is transmitted through both front and rear axles.

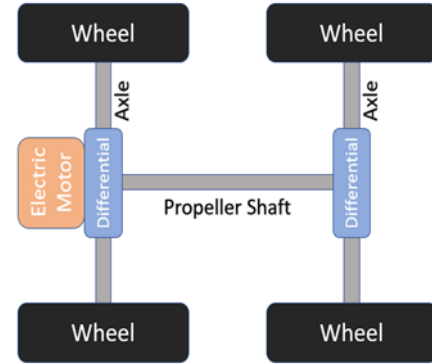


Figure 5. EM layout of AWD configuration

Eq. (1) is used to calculate the angular speed of the EM for F/RWD configurations [9].

$$\omega_{EM} = \int \frac{T_{EM} - T_w}{J_a + 4J_w + J_{EM}} \frac{dt}{i_d^2 \eta_d} \quad (1)$$

Eq. (2) is used to calculate the angular speed of the EM for AWD configurations. AWD power train has double axles. For this reason, an additional axle moment of inertia has been added to the F/RWD vehicle powertrain transfer function.

$$\omega_{EM} = \int \frac{T_{EM} - T_w}{2J_a + 4J_w + J_{EM} + J_s} \frac{dt}{i_d^2 \eta_d} \quad (2)$$

where ω_{EM} EM denotes the angular speed of the EM, T_{EM} denotes the torque of the EM, T_w denotes the torque of the wheel, J_{EM} denotes the mass moment of inertia of the EM, J_w denotes the mass moment of inertia of the wheel, J_a denotes the mass moment of the inertia of the axle, J_s denotes the mass moment of the inertia of the propeller shaft, i_d denotes the final drive reduction ratio, and η_d denotes the efficiency of the final drive.

2.4 Longitudinal Resistance Forces Subsystem

In this study, only longitudinal vehicle dynamics are considered. Neither active safety systems nor lateral/vertical vehicle dynamics are considered.

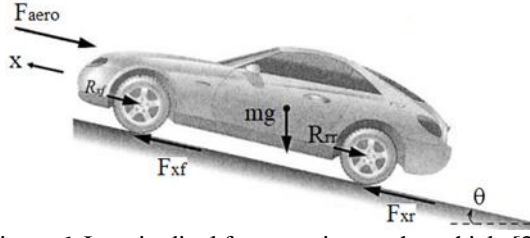


Figure 6. Longitudinal forces acting on the vehicle [34]

The external longitudinal forces acting on the vehicle that moves on an inclined road are aerodynamic drag forces, gravitational forces, longitudinal traction forces on tires, and rolling resistance forces [34].

$$F_i = F_{xf} + F_{xr} - F_{aero} - R_{xf} - R_{xr} - mgsin(\theta) \quad (3)$$

Total traction force (F_{tr}) can be expressed as the sum of the longitudinal traction forces at both front and rear tires.

$$F_{tr} = F_{xf} + F_{xr} \quad (4)$$

Also, the term of ' $mgsin(\theta)$ ' can be described as the gravitational load on the vehicle. Besides all these, aerodynamic drag force, rolling resistance force, and inertial force can be described as in Eq. (6).

$$F_{tr} = ma + \frac{1}{2}\rho C_d A_f (V + V_{wind})^2 + F_z C_{rr} \quad (5)$$

where F_{xf} denotes the longitudinal traction force at the front tires, F_{xr} denotes the longitudinal traction force at the rear tires, F_{aero} denotes the longitudinal aerodynamic drag force, R_{xf} denotes the force due to rolling resistance at the front tires, R_{xr} denotes the force due to rolling resistance at the rear tires, m denotes the mass of the vehicle, a denotes the acceleration of the vehicle, g denotes the gravitational acceleration, θ denotes the angle of inclination, F_i denotes the inertial force of the vehicle, ρ denotes the mass density of air, C_d denotes the aerodynamic drag coefficient, A_f denotes the projected frontal area of the vehicle in the direction of travel, V denotes the longitudinal vehicle velocity, V_{wind} denotes the wind velocity (positive for a headwind and negative for a tailwind), F_z denotes the normal force to the tire, and C_{rr} denotes the rolling resistance coefficient.

2.5 Battery Subsystem

The BEV models are equipped with a battery with a capacity of 80 kWh. The battery power is determined by dividing EM power by EM efficiency in order to obtain total energy consumption of the system (Accessory load is also considered). The obtained energy consumption data are utilized to calculate battery current, AEC, and SOC. Also, the initial value of SOC is determined as 90% to increase regenerative braking efficiency during the simulation.

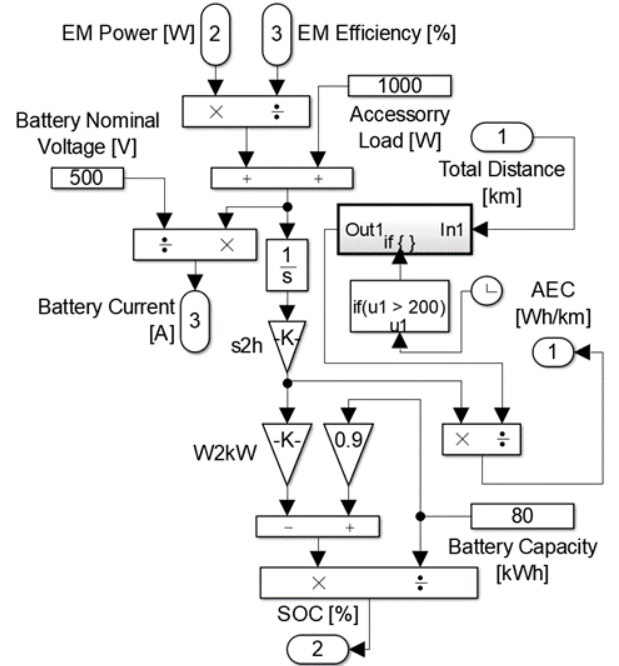


Figure 7. Battery Subsystem

2.6 Brake Subsystem

While the normal force distribution on the tires is being determined, the net pitch torque on the vehicle can be assumed as zero, which means that the pitch angle of the vehicle is assumed to reach a steady-state value [34].

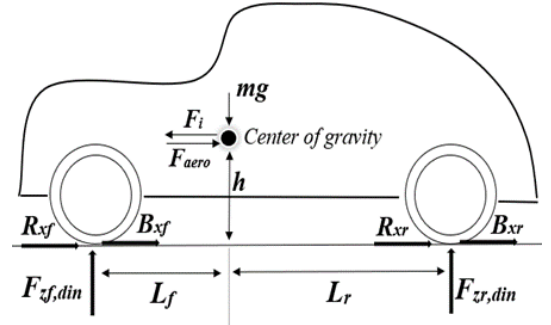


Figure 8. The normal force distribution on tires during braking

$F_{zf,din}$ is described by taking moments about the contact point of the rear tire (Fig. 8).

$$F_{zf,din} = \frac{mgL_r + h(F_i - F_{aero})}{L_f + L_r} \quad (10)$$

$F_{zr,din}$ is described by taking moments about the contact point of the front tire (Fig. 8).

$$F_{zr,din} = \frac{mgL_f + h(F_{aero} - F_i)}{L_f + L_r} \quad (11)$$

Maximum adhesion between front tires and road while braking is described as in Eq. (12).

$$B_{xf} = \mu F_{zf,din} \tag{12}$$

Maximum adhesion between rear tires and road while braking is described as in Eq. (13).

$$B_{xr} = \mu F_{zr,din} \tag{13}$$

where $F_{zf,din}$ denotes the normal force at the front tires, $F_{zr,din}$ denotes the normal force at the rear tires, B_{xf} denotes the maximum braking force at the front tires, B_{xr} denotes the maximum

braking force at the rear tires, L_f denotes the distance between front tires and center of gravity, L_r denotes the distance between rear tires and center of gravity, h denotes the height of the center of gravity, and μ denotes the adhesion coefficient of the wheels.

There are three different regenerative braking strategies for each configuration. For this reason, three different braking subsystems should be set.

In the colored areas, maximum adhesion between front/rear tires and road, which refers to the maximum braking force of the related tire, is calculated. Then, the actual braking force on the related tire is obtained by multiplying the BPP by the maximum braking force (Fig. 9).

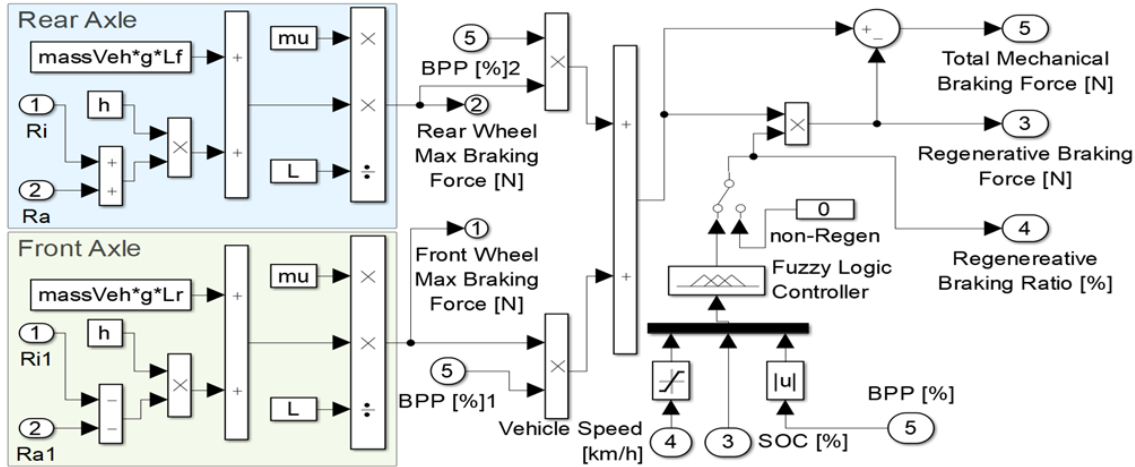


Fig. 9. AWD Brake Subsystem

Regenerative braking is only possible with the braking force on front wheels for FWD configuration and with the braking force on rear wheels for the RWD configuration. However, it is both possible with the braking force on the front and rear wheels for the AWD configuration.

Moreover, the fuzzy logic controller determines the regenerative braking ratio in all cases accurately, and this ratio is utilized to calculate the regenerative braking force.

A Mamdani fuzzy logic controller with three inputs and one output is created to determine the regenerative braking ratio. Input data of the fuzzy logic controller are determined as vehicle speed, SOC, and BPP. Moreover, the output of the fuzzy logic controller is determined as the regenerative braking ratio.

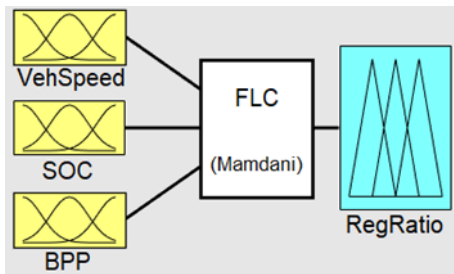


Figure 10. Fuzzy logic controller

For vehicle speed variable, membership functions are determined as low, medium, and high speeds in the range of 0-200 km/h. Vehicle speed has a significant effect on brake safety [14]. If the vehicle

speed is low, the regenerative braking ratio should also be low to ensure braking safety. If the vehicle speed is medium, the regenerative braking ratio can be increased correspondingly. The condition, where the vehicle speed is high, is determined as the optimum stage for regenerative braking.

For the SOC variable, membership functions are determined as a low, medium, and high in the range of 0-1. If SOC value is lower than 10%, the inner resistance of the battery has a high value, which is inappropriate for charging. For this reason, the regenerative braking ratio should be low at this stage. If SOC value is between 10% and 90%, it is the ideal situation to charge the battery with a large current, and the regenerative braking ratio should be increased correspondingly. If SOC value is higher than 90%, the regenerative braking ratio should be decreased to prevent the deposit of li-on [14]. For the BPP variable, membership functions are determined as low, medium, and high demands in the range of 0-1.

If braking demand is low, it is the optimum stage for regenerative braking. The EM can ensure most of the braking demand, and it enables high energy saving. If braking demand is high, a quick response should be provided to the system. For this reason, the majority of the braking force is supplied by mechanical braking. Furthermore, the regenerative braking ratio takes the lowest values at this stage. The medium braking demand is inferentially generated between these two stages. For the regenerative braking ratio variable, membership functions are determined as very low (VL), low (L), medium (M), high (H), and very high (VH) demands in the range of 0-1.

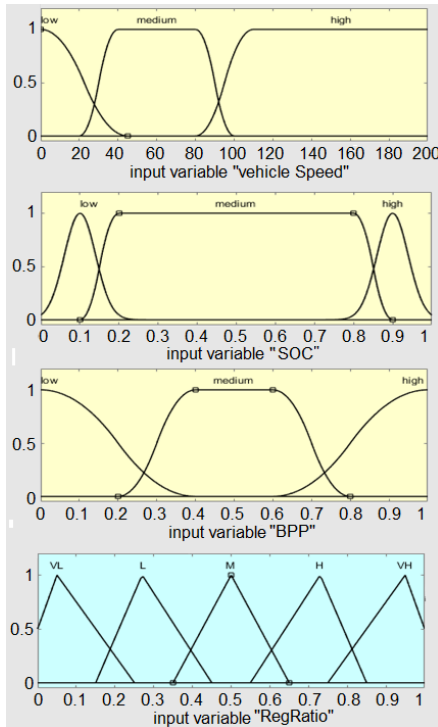


Figure 11. Membership Functions

Table 1. Fuzzy logic rule table

BPP (%)	SOC (%)	Vehicle Speed (km/h)	Regenerative Braking Ratio (%)
High	High	High	L
		Medium	L
		Low	VL
	Medium	High	M
		Medium	L
		Low	VL
	Low	High	L
		Medium	L
		Low	VL
Me- dium	High	High	M
		Medium	L
		Low	L
	Medium	High	VH
		Medium	H
		Low	H
	Low	High	M
		Medium	M
		Low	L
Low	High	High	M
		Medium	M
		Low	L
	Medium	High	VH
		Medium	VH
		Low	H
	Low	High	H
		Medium	M
		Low	L

corresponding to different values of these three input variables. The rules algorithm is the set of fuzzy rules to be used for inference, and thanks to these if-then rules, the response of the system in different situations can be determined.

In this study, each input variable has three different states, and the fuzzy logic rule table contains 27 if-then rules that include all combinations of these input variables. The fuzzy logic rules are created by considering the conditions of the input variables mentioned above. It also shows that experience is the most significant thing while working with fuzzy logic. The fuzzy logic rule algorithm (if-then rules) and related membership functions are given in Table 1 and Fig. 11, respectively.

2.7 Simulation Parameters

The specifications of the BEV models and the simulation parameters are given in Table 2. Vehicle parameters are taken from studies in the literature, vehicle and product catalogs. The same parameters were used for all vehicle structures examined in the study.

Table 2. BEV models and the simulation parameters

Parameters	Values
Mass of the vehicle	1850 kg
Battery capacity	80 kWh
Battery nominal voltage	500 V
Accessory load	1 kW
Wheel radius (r_w)	0.339 m
The frontal area of the vehicle	2.05 m ²
Aerodynamic drag coefficient (C_d)	0.27
Rolling resistance coefficient (C_{rr})	0.018
Adhesion coefficient (μ)	0.7
Gravitational acceleration (g)	9.81 m/s ²
Air density	1.1839 kg/m ³
Final drive ratio (reduction ratio) (i)	6
Inclination angle	0°
The efficiency of the final drive (η)	0.96
Height of the center of gravity (h)	0.45 m
Distance between rear tires and center of gravity (L_r)	1.5 m
Distance between front tires and center of gravity (L_f)	1.35 m
Mass moment of the wheel	1.15 kgm ²
Mass moment of the propeller shaft	0.55 kgm ²
Mass moment of the axle	0.5 kgm ²
Mass moment of EM	0.086 kgm ²

3. Results and Discussion

3.1 Distance, Speed, and Acceleration Graphs

In the first graph, reference/actual vehicle speed curves and in the second graph, acceleration data of the vehicle are shown (Fig. 12). Total distance, vehicle speed (1st graph), and acceleration (2nd graph) data are obtained from the EM speed data, which is calculated in the Driveline Subsystem. As it is seen in the first graph, reference speed overlaps with the actual vehicle speed, which affirms the truth of the others (Fig 12).

A fuzzy logic rule algorithm is created to determine output states

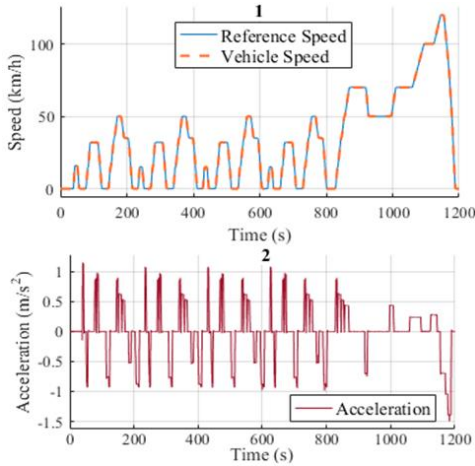


Figure 12. Speed and acceleration graphs (NEDC)

The vehicle reaches to 11 km in NEDC, 23.3 km in WLTP Class 3, and 17.77 km in FTP-75. Moreover, the average speed of the vehicle is 33.6 km/h in NEDC, 46.5 km/h in WLTP Class 3, and 34.1 km/h in FTP-75 (Table 3).

Also, the operating time of NEDC is 1200 seconds, WLTP Class 3 is 1800 seconds, and FTP-75 is 1874 seconds.

Table 3. Specifications of driving cycles

	Total Distance (km)	Maximum Speed (km/h)	Average Speed (km/h)
NEDC	11	120	33.6
WLTP Class 3	23.3	131.3	46.5
FTP-75	17.77	91.25	34.1

3.2 Distance, Speed, and Acceleration Graphs

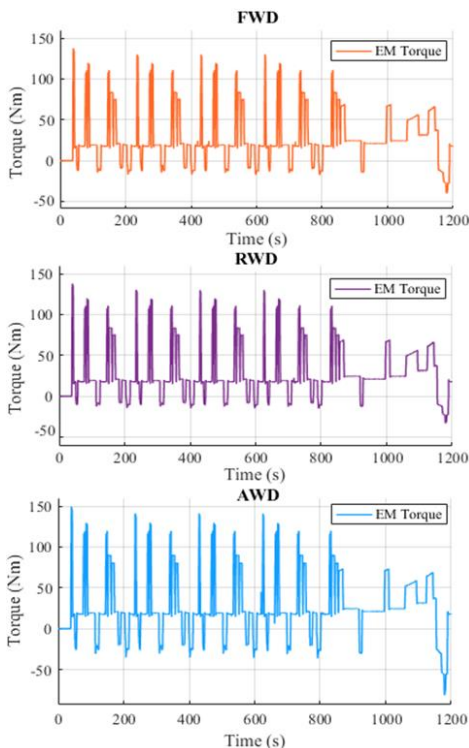


Figure 13. EM Torque graphs (NEDC)

EM torque graphs for FWD, RWD, and AWD models are shown in the first, second, and third lines, respectively (Fig. 13).

EM torque depends on APP and BPP values. When the pedal position is greater than 0, which is driving mode, EM torque takes positive values. When the pedal position is smaller than 0, which is the braking mode, EM torque takes negative values proportional to the regenerative braking ratio. As it is seen in Fig. 13, the driving time is considerably more than the regenerative braking time. EM power and battery current also take negative values during regenerative braking.

Given regenerative braking times, the FWD model has a relatively more regenerative braking time than the RWD model. In contrast, the AWD model has a considerably more regenerative braking time than both.

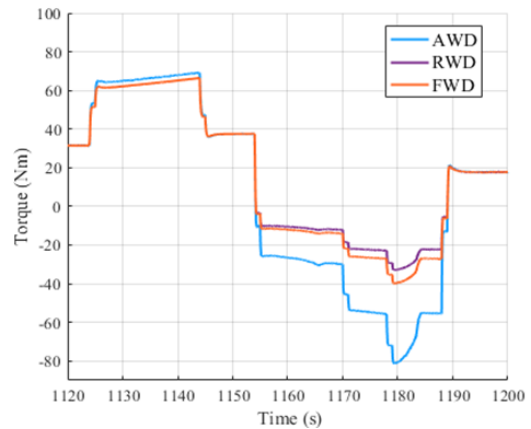


Figure 14. EM Torque comparison (NEDC)

In Fig. 14, EM Torque curves for FWD, RWD, and AWD configurations are given in the same graph. Only the last 80 seconds of the simulation are considered in order to make the graph more understandable. As can be seen from this comparative graph, FWD and RWD configurations have the same values during the driving mode. However, the FWD configuration is more effective than the RWD configuration during regenerative braking. Besides, the AWD configuration sometimes takes different values during the driving mode because of its driveline equation is different from the others. Furthermore, AWD configuration is quite active during regenerative braking compared to the others.

3.3 Regenerative/Mechanical Braking Forces Graphs

Regenerative braking force (RBF) graphs for FWD, RWD, and AWD models are shown in the first, second, and third lines, respectively (Fig. 15).

As it is seen in Fig. 15, the FWD model has a relatively higher RBF than the RWD model. In comparison, the AWD model has a considerably higher RBF than both, which means AWD configuration has a more significant proportion of regenerative braking during braking compared to FWD and RWD configurations.

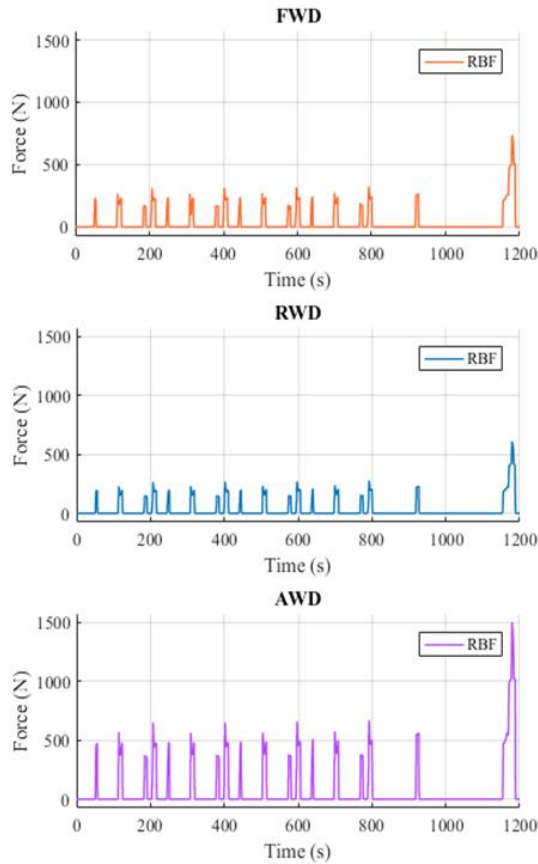


Figure 15. Regenerative Braking Forces graphs (NEDC)

In Fig. 16, RBF curves for FWD, RWD, and AWD configurations are given in the same graph. Only the last one-third of the simulation is considered in order to make the graph more understandable. As can be seen from this comparative graph, the maximum RBF observed during braking for the FWD configuration is approximately 735 N, for the RWD configuration approximately 605 N, and for the AWD configuration approximately 1500 N. Also, average force values during regenerative braking are ordered from the highest to the smallest as AWD, FWD, and RWD models.

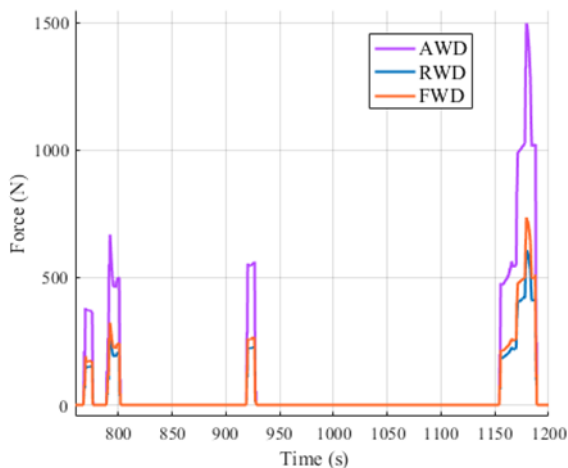


Figure 16. Regenerative Braking Forces comparison (NEDC)

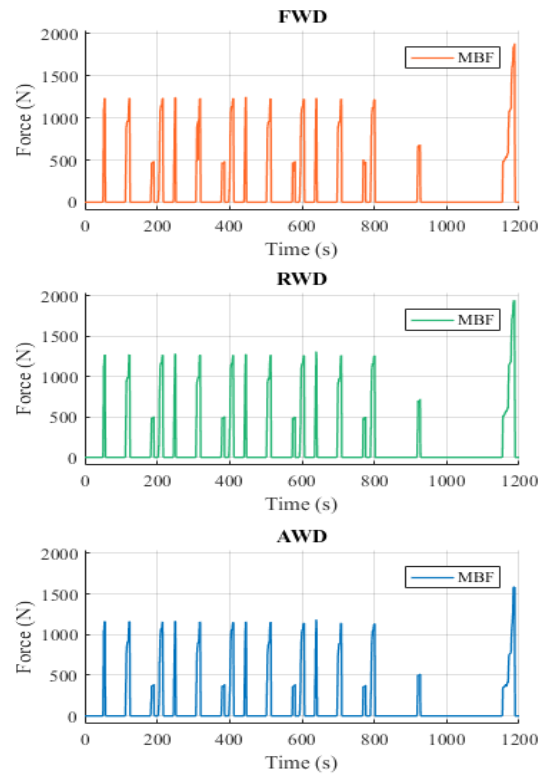


Figure 17. Mechanical Braking Forces graphs (NEDC)

Mechanical braking force (MBF) graphs for FWD, RWD, and AWD models are shown in the first, second, and third lines, respectively (Fig. 17).

As it is seen in Fig. 17, AWD configuration has the smallest proportion of mechanical braking while braking compared to FWD and RWD configurations. Moreover, the RWD model has a higher MBF than both, which means RWD configuration has a more significant proportion of mechanical braking during braking compared to FWD and AWD configurations.

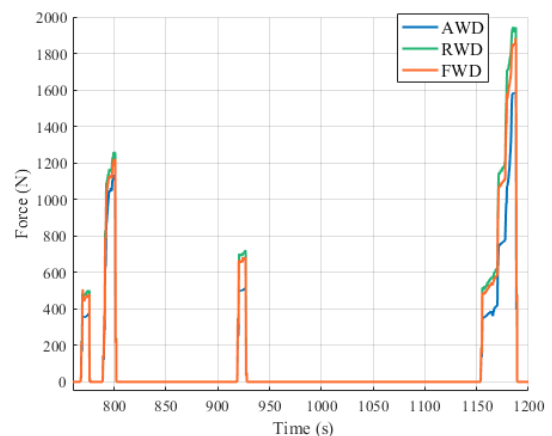


Fig. 18. Mechanical Braking Forces comparison (NEDC)

In Fig. 18, MBF curves for FWD, RWD, and AWD configurations are given in the same graph. Only the last one-third of the simulation is considered in order to make the graph more understandable. As can be seen from this comparative graph, the maximum MBF observed during braking for the FWD configuration is approximately 1850 N, for the RWD configuration 1950 N, and for the

AWD configuration 1600 N. Also, average force values during mechanical braking are ordered from the highest to the smallest as RWD, FWD, and AWD models.

3.4 State of Charge Graphs

In Fig. 19, SOC values of both regenerative and non-regenerative configurations of FWD, RWD, and AWD models are shown. Only the last part of the simulation is considered in order to make the graph more understandable.

As a result of the driving cycles, models with regenerative braking are significantly more economical in terms of energy consumption compared to non-regenerative models.

As it is seen in Fig. 19, the most outstanding energy saving is accomplished in the AWD model. The non-regenerative configurations of the FWD and RWD models have the same results, while the FWD model has slightly better energy consumption characteristics than the RWD model in regenerative braking configurations.

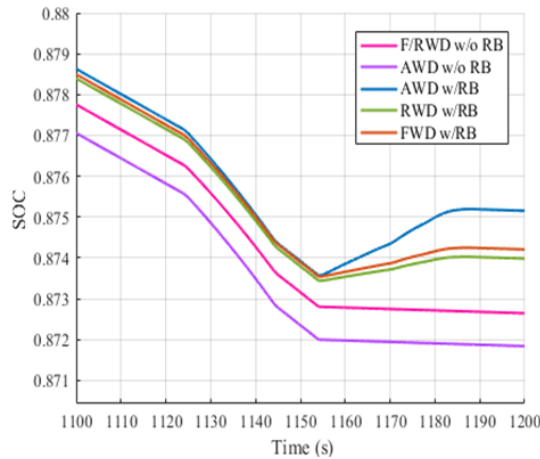


Fig. 19. SOC comparison (NEDC)

3.5 Range and Average Energy Consumption Comparison

Although it is an unhealthy condition for the battery, the system was operated until the SOC value reached 0% from 100% in order to consider the effectiveness of the fuzzy logic-based regenerative braking in any case.

In this period, the distances traveled by the models are determined, and these distances are called as their driving ranges. Also, the AECs of the models are calculated by dividing the battery capacity by the distance traveled.

Table 4. Range and AEC comparison (NEDC)

	w/RB		w/o RB	
	Range (km)	AEC (Wh/km)	Range (km)	AEC (Wh/km)
FWD	435.7	183.61	403.08	198.47
RWD	430.8	185.71	403.08	198.47
AWD	463.25	172.69	391.56	204.31

Under NEDC, the AEC of AWD is calculated as 172.69 Wh/km for regenerative configuration and 204.31 Wh/km for non-regenerative configuration. The AEC of FWD is calculated as 183.61 Wh/km

for regenerative configuration and 198.47 Wh/km for non-regenerative configuration.

The AEC of RWD is calculated as 185.71 Wh/km for regenerative configuration and 198.47 Wh/km for non-regenerative configuration (Table 4).

Under NEDC, the range of AWD is calculated as 463.25 km for regenerative configuration and 391.56 km for non-regenerative configuration. The range of FWD is calculated as 435.7 km for regenerative configuration and 403.08 km for non-regenerative configuration. The range of RWD is calculated as 430.8 km for regenerative configuration and 403.08 km for non-regenerative configuration (Table 4).

Table 3. Range and AEC comparison (WLTP Class 3)

	w/RB		w/o RB	
	Range (km)	AEC (Wh/km)	Range (km)	AEC (Wh/km)
FWD	424.13	188.62	386.56	206.95
RWD	417.92	191.42	386.56	206.95
AWD	458.22	174.59	374.74	213.48

Under WLTP Class 3, the AEC of AWD is calculated as 174.59 Wh/km for regenerative configuration and 213.48 Wh/km for non-regenerative configuration. The AEC of FWD is calculated as 188.62 Wh/km for regenerative configuration and 206.95 Wh/km for non-regenerative configuration. The AEC of RWD is calculated as 191.42 Wh/km for regenerative configuration and 206.95 Wh/km for non-regenerative configuration (Table 5).

Under WLTP Class 3, the range of AWD is calculated as 458.22 km for regenerative configuration and 374.74 km for non-regenerative configuration. The range of FWD is calculated as 424.13 km for regenerative configuration and 386.56 km for non-regenerative configuration. The range of RWD is calculated as 417.92 km for regenerative configuration and 386.56 km for non-regenerative configuration (Table 5).

Table 6. Range and AEC comparison (FTP-75)

	w/RB		w/o RB	
	Range (km)	AEC (Wh/km)	Range (km)	AEC (Wh/km)
FWD	440.8	181.49	388.76	205.78
RWD	431.2	185.52	388.76	205.78
AWD	489.67	163.38	373.9	213.96

Under FTP-75, the AEC of AWD is calculated as 163.38 Wh/km for regenerative configuration and 213.96 Wh/km for non-regenerative configuration. The AEC of FWD is calculated as 181.49 Wh/km for regenerative configuration and 205.78 Wh/km for non-regenerative configuration.

The AEC of RWD is calculated as 185.52 Wh/km for regenerative configuration and 205.78 Wh/km for non-regenerative configuration (Table 6).

Under FTP-75, the range of AWD is calculated as 489.67 km for regenerative configuration and 373.9 km for non-regenerative configuration. The range of FWD is calculated as 440.8 km for regenerative configuration and 388.76 km for non-regenerative configuration. The range of RWD is calculated as 431.2 km for regenerative

configuration and 388.76 km for non-regenerative configuration (Table 6).

4. Conclusions

In this study, the regenerative braking effectiveness of three different BEVs with different powertrains (FWD, RWD, and AWD) was determined by simulation. Besides, non-regenerative configurations of these systems were utilized for comparison. Various values, such as the driving range, AEC, and SOC, were obtained.

When comparing regenerative configurations with non-regenerative configurations, the energy-saving amounts are ordered from the best to the worst as AWD, FWD, and RWD models.

Under NEDC, 15.48% energy saving in the AWD model, 7.49% in the FWD model, and 6.43% in the RWD model were observed. Thanks to the fuzzy logic-based regenerative braking strategy, 71.69 km extra range in the AWD model, 32.62 km in the FWD model, and 27.72 km in the RWD model were observed.

Under WLTP Class 3, energy saving in the AWD model is 18.22%, in the FWD model is 8.86%, and in the RWD model is 7.5%. Moreover, additional range supplied by regenerative braking is 83.48 km in AWD, 37.57 km in FWD, and 31.36 km in RWD models.

Under FTP-75, energy saving in the AWD model is 23.64%, in the FWD model is 11.8%, and in the RWD model is 9.85%. Moreover, additional range supplied by regenerative braking is 115.77 km in AWD, 52.04 km in FWD, and 42.44 km in RWD models.

The arithmetic mean of the energy-saving values, which is supplied by fuzzy logic-based regenerative braking, in these three driving cycles is calculated.

Consequently, the mean energy-saving in AWD configuration is calculated as 19.11%, in FWD configuration is calculated as 9.38%, and in RWD configuration is calculated as 7.93%.

The reason why the FWD model has higher energy-saving potential than the RWD model is that the braking force on the front axle is greater than the braking force on the rear axle. Therefore, the RBF is higher in the FWD model.

Also, the AWD model naturally has a higher energy-saving potential than the other two models since the braking force on both axles can be used in regenerative braking on the AWD model.

As with any modeling, there are certain assumptions and neglected parameters in this study in order to simplify the models as much as possible, with a small amount of error.

In order to improve this study;

- A more advanced battery subsystem can be created by considering factors such as battery temperature and battery voltage as dependent variables.

- Vertical/lateral vehicle dynamics and active driving safety systems can be considered. Thus, an inclined driving cycle can be created and applied.

- Driving cycles have relatively low acceleration and low braking demands. The effect of the fuzzy logic-based regenerative braking system can be better analyzed by creating an advanced braking scenario.

- The regenerative braking ratio, which is the output of the fuzzy logic controller, can be defined more gradually. Also, the fuzzy rules table can be developed by investigating various braking situations.

- In the FWD, RWD, and AWD configurations, the exact location

of the vehicles' center of gravity can be explored.

Nomenclature

NEDC	New European Driving Cycle
WLTP	Worldwide Harmonised Light Vehicles Test Procedure
FTP-75	Federal Test Procedure
BEV	Battery Electric Vehicle
EM	Electric Motor
FWD	Front-Wheel Drive
RWD	Rear-Wheel Drive
AWD	All-Wheel Drive
BPP	Brake Pedal Position
APP	Accelerator Pedal Position
AEC	Average Energy Consumption
SOC	State of Charge
RB	Regenerative Braking
RBF	Regenerative Braking Force
MBF	Mechanical Braking Force
W/	With...
W/O	Without...

Conflict of Interest Statement

The authors declare that there is no conflict of interest.

CRedit Author Statement

Enes Yurdaer: Methodology, Data curation, Writing - review & editing, **Tolga Kocakulak:** Conceptualization, Supervision, Writing - review & editing, Validation

References

1. Ekici, Y. E., & Nusret, T. A. N. (2019). Charge and dis-charge characteristics of different types of batteries on a hybrid electric vehicle model and selection of suitable battery type for electric vehicles. *International Journal of Automotive Science and Technology*, 3(4), 62-70. <https://doi.org/10.30939/ijastech..527971>
2. Kunt, M. A. (2020). Advisor Based Modelling of Regenerative Braking Performance of Electric Vehicles at Different Road Slopes. *International Journal of Automotive Science and Technology*, 4(2), 98-104. <https://doi.org/10.30939/ijastech..717097>
3. Un-Noor, F., Padmanaban, S., Mihet-Popa, L., Mollah, M.N., Hossain, E. (2017). A Comprehensive Study of Key Electric Vehicle (EV) Components, Technologies, Challenges, Impacts, and Future Direction of Development. *Energies*, 10, 1217. <https://doi.org/10.3390/en10081217>
4. Kiyaklı, A. O., & Solmaz, H. (2018). Modeling of an Electric Vehicle with MATLAB/Simulink. *International Journal of Automotive Science And Technology*, 2(4), 9-15. <https://doi.org/10.30939/ijastech.475477>
5. D. U. Thakar and R. A. Patel (2019). Comparison of Advance and Conventional Motors for Electric Vehicle Application, 2019 3rd International Conference on Recent Developments in Control, Automation & Power Engineering (RDCAPE), NOIDA, India, pp. 137-142, doi: 10.1109/RDCAPE47089.2019.8979092.
6. J. Ruan and Q. Song (2019). A Novel Dual-Motor Two-Speed Direct Drive Battery Electric Vehicle Drivetrain, in *IEEE Access*, vol. 7, pp. 54330-54342, doi: 10.1109/ACCESS.2019.2912994.
7. C. A. Bilatiu, S. I. Cosman, R. A. Martis, C. S. Martis and S. Morariu,

- (2019). Identification and Evaluation of Electric and Hybrid Vehicles Propulsion Systems. 2019 Electric Vehicles International Conference (EV). doi:10.1109/ev.2019.8892965
8. Ghasri, M., Ardeshiri, A., & Rashidi, T. (2019). Per-ceived Advantage in Perspective Application of Integrat-ed Choice and Latent Variable Model to Capture Electric Vehicles Perceived Advantage from Consumers Perspec-tive. arXiv preprint arXiv:1905.11606.
 9. Kocakulak, T., & Solmaz, H. (2020). HCCI Menzil Art-tirici Motor Kullanilan Seri Hibrit Bir Aracin Modellen-mesi. Gazi Üni-versitesi Fen Bilimleri Dergisi Part C: Tasarım Ve Teknoloji, 8(2), 279-292. <https://doi.org/10.29109/gujsc.670564>
 10. M. K. Yoong, Y. H. Gan, G. D. Gan, & K.W Chew. (2010). "Studies of regenerative braking in electric vehi-cle," 2010 IEEE Conference on Sustainable Utilization and Development in Engineering and Technology, Petal-ing Jaya, pp. 40-45, doi: 10.1109/STUDENT.2010.5686984.
 11. Heydari, S., Fajri, P., Rasheduzzaman, M., & Sabzehgar, R. (2019). Maximizing regenerative braking energy re-recovery of electric vehicles through dynamic low-speed cutoff point detection. IEEE Transactions on Transpor-tation Electrification, 5(1), 262-270.
 12. Heydari, S., Fajri, P., Sabzehgar, R., & Rasouli, M. (2019). A Novel Approach for Maximizing Regenerative Braking Energy Extraction of Electric Vehicles Using Motor Performance Lookup Table. In 2019 IEEE Trans-portion Electrification Conference and Expo (ITEC) (pp. 1-5). IEEE. DOI: 10.1109/ITEC.2019.8790633
 13. Heydari, S., Fajri, P., Sabzehgar, R., & Asrari, A. (2020). Optimal Brake Allocation in Electric Vehicles for Maxim-izing Energy Harvesting During Braking. IEEE Transac-tions on Energy Conversion. DOI: 10.1109/TEC.2020.2994520
 14. J. Paterson and M. Ramsay (1993). "Electric vehicle braking by fuzzy logic control," Conference Record of the 1993 IEEE Industry Applications Conference Twen-ty-Eighth IAS Annual Meeting, Toronto, Ontario, Cana-da, pp. 2200-2204 vol.3, doi: 10.1109/IAS.1993.299173.
 15. Liu, H., Lei, Y., Fu, Y., & Li, X. (2020). An Optimal Slip Ratio-Based Revised Regenerative Braking Control Strategy of Range-Extended Electric Vehi-cle. Energies, 13(6), 1526. <https://doi.org/10.3390/en13061526>
 16. Zhao, W., Wu, G., Wang, C., Yu, L., & Li, Y. (2019). Energy transfer and utilization efficiency of regenerative braking with hybrid energy storage system. Journal of Power Sources, 427, 174-183. <https://doi.org/10.1016/j.jpowsour.2019.04.083>
 17. Totev, V., Gueorgiev, V., & Rizov, P. (2019). Regenera-tive braking of electric vehicles. In 2019 11th Electrical Engineering Faculty Conference (BuleF) (pp. 1-5). IEEE.
 18. Zhao, X., Li, L., Wang, X., Mei, M., Liu, C., & Song, J. (2019). Braking force decoupling control without pres-sure sensor for a novel series regenerative brake sys-tem. Proceedings of the Institution of Mechanical Engi-neers, Part D: Journal of Automobile Engineer-ing, 233(7), 1750-1766. <https://doi.org/10.1177/2F0954407018785740>
 19. C. Qiu, G. Wang, M. Meng, and Y. Shen (2018). A nov-el control strategy of regenerative braking system for electric vehicles under safety critical driving situations, Energy 149, 329 – 340. <https://doi.org/10.1016/j.energy.2018.02.046>
 20. S. Oleksowicz, K. Burnham, and A. Gajek (2012). On the legal, safety and control aspects of regenerative brak-ing in hybrid/electric vehicles.
 21. Martellucci, L., & Giannini, M. (2020). Regenerative Braking Experimental Tests and Results for Formula Student Car. Journal of Transportation Technologies, 11(1), 78-89. <https://doi.org/10.4236/jtts.2021.111005>
 22. Subramaniam, K. V., & Subramanian, S. C. (2021). Impact of regen-erative braking torque blend-out characteristics on electrified heavy road vehicle braking performance. Vehicle System Dynamics, 59(2), 269-294. <https://doi.org/10.1080/00423114.2019.1677921>
 23. De Pinto, S., Camocardi, P., Chatzikomis, C., Sorniotti, A., Bottiglione, F., Mantriota, G., & Perlo, P. (2020). On the comparison of 2-and 4-wheel-drive electric vehicle layouts with central motors and single-and 2-speed transmission systems. Energies, 13(13), 3328. <https://doi.org/10.3390/en13133328>
 24. Ju, F., Zhuang, W., Wang, L., & Zhang, Z. (2020). Comparison of four-wheel-drive hybrid powertrain configurations. Energy, 118286. Ju, F., Zhuang, W., Wang, L., & Zhang, Z. (2020). Comparison of four-wheel-drive hybrid powertrain configurations. Energy, 118286. <https://doi.org/10.1016/j.energy.2020.118286>
 25. Tan, F., & Yan, E. (2020). An Efficiency-Based Hybrid Mode Selection Model for A P134 Plug-In Hybrid Powertrain Architecture (No. 2020-01-5001). SAE Technical Paper. <https://doi.org/10.4271/2020-01-5001>
 26. J. Zhang, B. Song, S. Cui and D. Ren (2009). "Fuzzy Logic Approach to Regenerative Braking System," 2009 International Conference on Intelligent Human-Machine Systems and Cybernetics, Hangzhou, Zhejiang, pp. 451-454, doi: 10.1109/IHMISC.2009.120.
 27. X. Guoqing, L. Weimin, X. Kun & Song, Zhibin. (2011). An Intelligent Regenerative Braking Strategy for Electric Vehicles. Energies. 4. 1461-1477. 10.3390/en4091461.
 28. Maia R., Silva M., Araùjo R., Nunes U. (2015). Electri-cal vehicle modeling : a Fuzzy logic model for regenerative braking. Expert Systems with Applications. Volume 42, Issue 22. <https://doi.org/10.1016/j.eswa.2015.07.006>
 29. Y. Tao, X. Xie, H. Zhao, W. Xu and H. Chen (2017). A regenerative braking system for electric vehicle with four in-wheel motors based on fuzzy control. 2017 36th Chi-nese Control Conference (CCC), Dalian, pp. 4288-4293, doi: 10.23919/ChiCC.2017.8028032.
 30. Xiao, Boyi & Lu, Huazhong & Wang, Hailin & Ruan, Jiageng & Zhang, Nong. (2017). Enhanced Regenerative Braking Strategies for Electric Vehicles: Dynamic Per-formance and Potential Analysis. Energies. 10. 1875. 10.3390/en10111875.
 31. Xin, Yafei & Zhang, Tiezhu & Zhang, Hongxin & Zhao, Qinghai & Zheng, Jian & Wang, Congcong. (2019). Fuzzy Logic Optimization of Composite Brake Control Strategy for Load-Isolated Electric Bus. Mathematical Problems in Engineering. 2019. 1-14. 10.1155/2019/9735368.
 32. Kocakulak, T., & Solmaz, H. (2020). Control of pre and post transmis-sion parallel hybrid vehicles with fuzzy log-ic method and comparison with other power sys-tems. Journal of the Faculty of Engineering and Architec-ture of Gazi University, 35(4), 2269-2286. DOI:10.17341/gazimmfd.709101
 33. HVH 250-115 Electric Motor datasheet. https://cdn.borgwarner.com/docs/default-source/default-document-library/remy-pds---hvh250-115-sheet-euro-pr-3-16.pdf?sfvrsn=ad42cd3c_11, last access date: 13.08.2020
 34. R. Rajamani (2011). Vehicle dynamics and control, Mechanical Engi-neering Series, Springer US.